

Figure 8 Fabricated resonator with $a = 2$ mm, $b = 14$ mm, $l = 8.5$ mm, and measured insertion loss. (a) Fabricated resonator and (b) insertion loss. [Color figure can be viewed in the online issue, which is available at wileyonlinelibrary.com]

resonator, respectively, by applying correction factor to calibrate the tolerance of the calculated resonant frequency. The open-ended coaxial cavity resonator suggested and designed in the study expects to be implied in many fields of measuring the frequency such as dielectric constant sensor, moisture sensor and so forth by using the characteristics of changing in resonant frequency and quality value as the amount of dielectric on the open side of the resonator varies.

REFERENCES

1. D.J. Barker, P.M. Suherman, T.J. Jackson, and M.J. Lancaster, Comparison of scanning evanescent microwave microscopy with coplanar waveguide methods of characterization of Ba_{0.5}Sr_{0.5}TiO₃ thin films, In: 18th IEEE International Symposium on the Applications of Ferroelectric, ISAF 2009, 2009.
2. S. Nakayama, Development of a microwave moisture sensor for aggregates, *Meas Sci Technol* 6 (1995), 429–431.
3. U. Raveendranath, S. Bijukumar, and K.T. Mathew, Broadband coaxial cavity resonator for complex permittivity measurements of liquids, *IEEE Trans Instrum Meas* 49 (2000), 1305–1312.
4. B.A. Galwas, J.K. Piotrowski, and J. Skulski, Dielectric measurements using a coaxial resonator opened to a waveguide below cut-off, *IEEE Trans Instrum Meas* 46 (1997), 511–514.
5. D.K. Cheng, *Field and wave electromagnetics*, Addison-Wesley, Reading, MA, 1961.
6. D.M. Pozar, *Microwave engineering*, 3rd ed., Wiley, New York, 1998.

© 2014 Wiley Periodicals, Inc.

A PLANAR COMPACT METAMATERIAL-INSPIRED BROADBAND ANTENNA

Anila P V,¹ Indhu K K,¹ Nijas C M,¹ Sujith R,¹ Mridula S,² and P Mohanan¹

¹Centre for Research in Electromagnetics and Antennas (CREMA), Department of Electronics, Cochin University of Science and Technology, Cochin 22, Kerala, India; Corresponding author: drmoohan@gmail.com

²School of Engineering, Cochin University of Science and Technology, Cochin 22, Kerala, India

Received 26 June 2013

ABSTRACT: An electrically small, broadband-modified, truncated ground metamaterial EZ antenna is presented. This, a modified EZ antenna system, achieves a larger bandwidth of the order of 650 MHz by adjusting the metamaterial-inspired meandered ground element fed by a top loaded monopole. The design is devoid of the large ground planes and the external parasitic elements used in conventional designs for achieving proper impedance matching characteristics. The antenna requires a small foot print of $\lambda_g/15 \times \lambda_g/10$, where λ_g is the guided wavelength corresponding to the lowest frequency of operation, when printed on a substrate of dielectric constant 4.4 and thickness 1.6 mm. The antenna offers a 2:1 VSWR bandwidth from 750 MHz to 1.4 GHz, which covers CDMA, GSM, and ISM bands. © 2014 Wiley Periodicals, Inc. *Microwave Opt Technol Lett* 56:610–613, 2014; View this article online at wileyonlinelibrary.com. DOI 10.1002/mop.28175

Key words: broadband antenna; electrically small antenna; metamaterial antenna; planar antenna

1. INTRODUCTION

The demand for portable mobile devices is increasing progressively with the development of novel wireless communication techniques. An inexpensive, easy to fabricate, efficient, and electrically small antenna (ESA) system would be an ideal choice for many new generation slim communication gadgets. The increased use of wireless technologies for various purposes strengthens the desire to achieve such an environment with a new paradigm of metamaterials [1]. Its classification, designs, and applications are discussed elaborately in [2]. A resonant hybrid radiating system can be obtained with proper combination of metamaterial element and radiating system. A variety of metamaterial-based and metamaterial-inspired designs have been reported in [3–8].

2. ANTENNA GEOMETRY

The geometry of the proposed antenna fabricated on a substrate of dielectric constant (ϵ_r) 4.4 and thickness (h) 1.6 mm is shown in Figure 1. A conventional monopole top loaded with a stub of length L_5 and width W_2 is symmetrically placed on the other side of the meandered ground plane. The width of each meander line (W_1) is 5 mm, while the bottom ground width L_1 is maintained at 12 mm. Similarly, length of each vertical meander line (L_3) is 4.2 mm except for L_2 , which is 4 mm. All the dimensions are critical and are optimized to get the maximum bandwidth for a compact, low-profile antenna. The optimum condition is achieved when the monopole is aligned to the centre. The side view and photograph of the top and bottom view of the proposed compact antenna are shown in Figures 1(b) and 1(c), respectively.

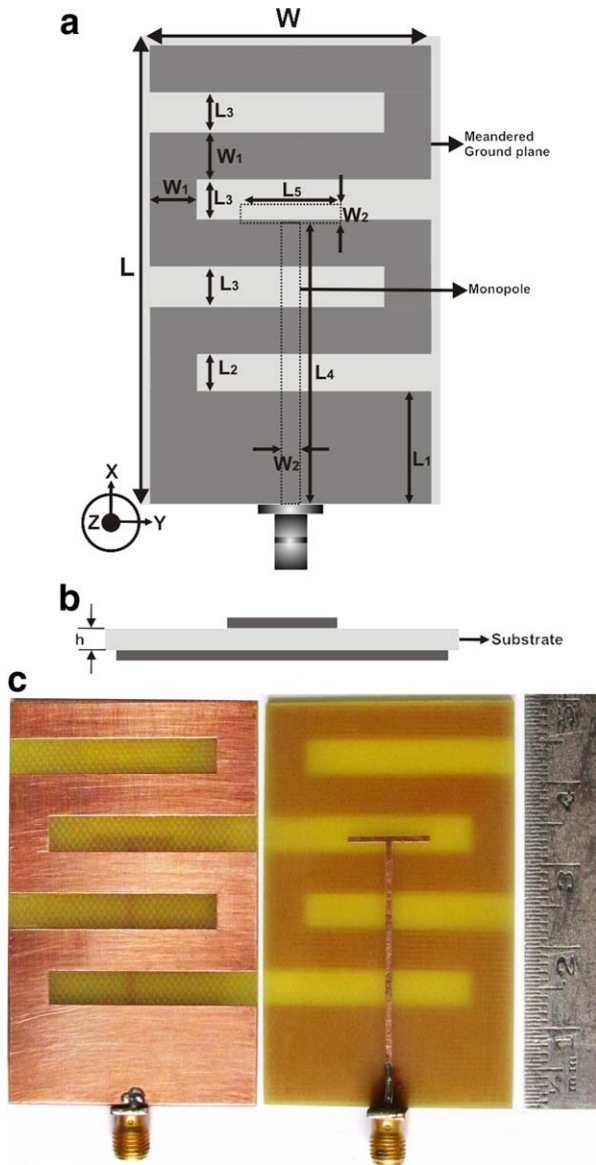


Figure 1 (a, b) Geometry of the proposed antenna ($L = 50$ mm, $W = 30$ mm, $L_1 = 12$ mm, $L_2 = 4$ mm, $L_3 = 4.2$ mm, $L_4 = 31.5$ mm, $L_5 = 10$ mm, $W_1 = 5$ mm, $W_2 = 0.6$ mm, $h = 1.6$ mm, $\epsilon_r = 4.4$) and (c) Photograph of the proposed compact antenna. [Color figure can be viewed in the online issue, which is available at wileyonlinelibrary.com]

3. RESULTS AND DISCUSSIONS

The simulation and the experimental studies were done using Ansoft HFSS and HP8510C Network analyzer, respectively. The simple monopole is top loaded with a rectangular strip to improve the impedance match of the antenna without much alteration in the resonant frequency.

In order to achieve a compact, low-frequency antenna, a metamaterial-inspired meandered element is introduced on the other side of the top-loaded monopole. The structure of the final antenna is shown in Figure 1, and the measured and simulated reflection characteristics are shown in Figure 2. The prototype is a variation of conventional metamaterial ESA reported. However, here the antenna is optimized for broadband operation at lower frequencies without any external matching network. Low-frequency analysis of the proposed system was a tedious task giving a slight variation in its measured and simulated results.

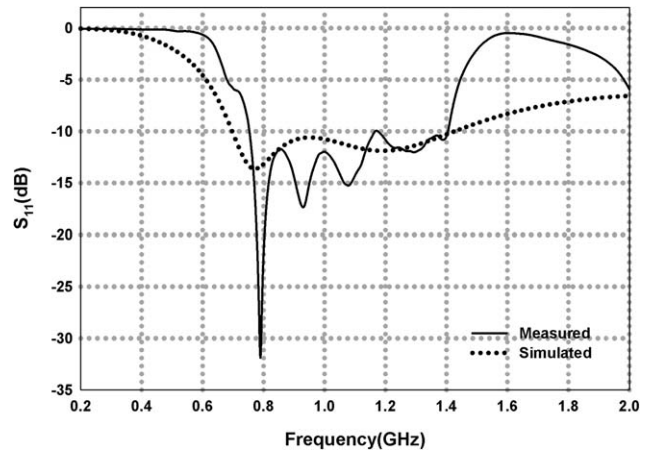


Figure 2 Reflection coefficient of the proposed antenna

It is observed that the broadband operation is achieved by merging different resonances. These resonances are due to the monopole and length of the meandering element. The antenna is compact and electrically small (with $K_a = 0.785$) for the lower end of frequencies. The antenna has a 2:1 VSWR bandwidth of 60.5% from 750 MHz to 1.4 GHz which covers CDMA (824–894 MHz), GSM 800(880–960 MHz), and ISM 900(902–928 MHz) communication bands. The proposed antenna system is devoid of external lumped elements and extra ground planes and matching circuits. So it can be integrated easily to any other systems.

Extensive parametric analysis has been carried out to find out the effect of each antenna parameter on the radiation performance.

The effect of monopole width on return loss of the antenna is shown in Figure 3. It is observed that the monopole width only affects the bandwidth of the antenna system as it reduces the matching, keeping the resonances almost the same. So the optimized width of the monopole is selected as 0.6 mm to balance with the reactance of the meander lines. The effects of monopole length on antenna return loss are shown in Figure 4. The high-frequency region is greatly affected by the length of the monopole more than the lower frequency region. It shifts gradually toward the lower side as monopole length increases. The periodicity (number of meandering segments) in the

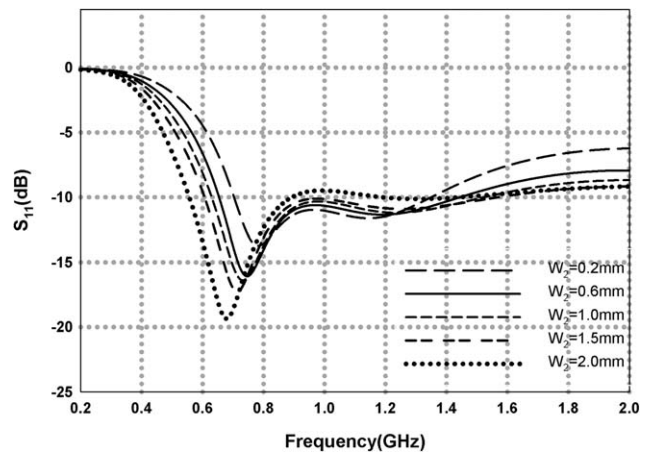


Figure 3 Variation of S_{11} with monopole width

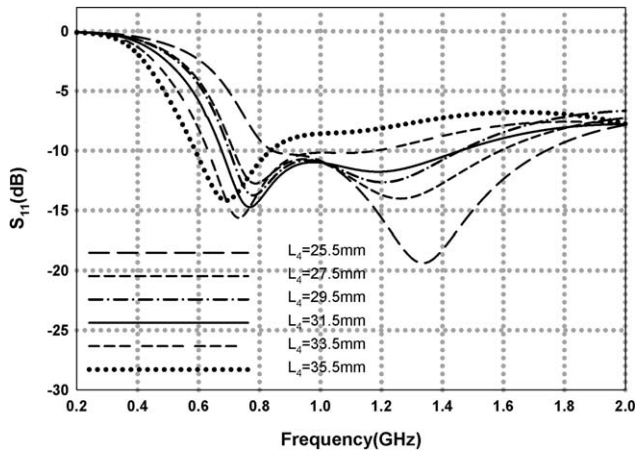


Figure 4 Variation of S_{11} with monopole length

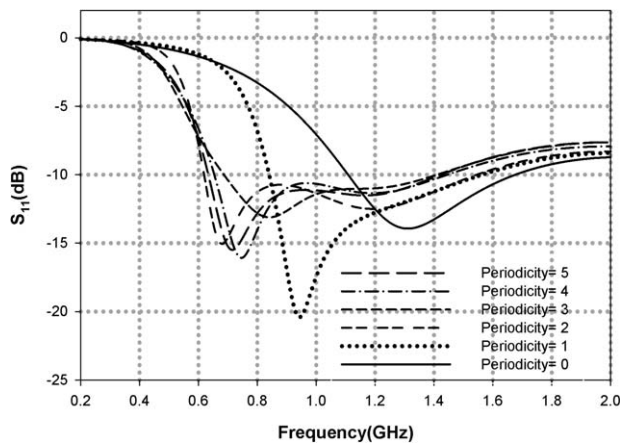


Figure 5 Variation of S_{11} with periodicity of meandering segments

proposed antenna is 4. Figure 5 shows the effect of the periodicity on S_{11} . It is inferred that the periodicity of meandering segments has a critical effect on the lower resonant frequency. As the number of meandering segments increases, the bandwidth also increases. Antenna structure can be truncated for any

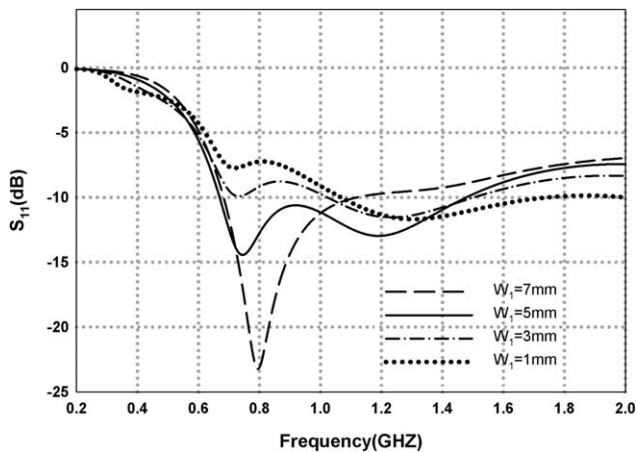


Figure 6 Variation of S_{11} with width of meander line

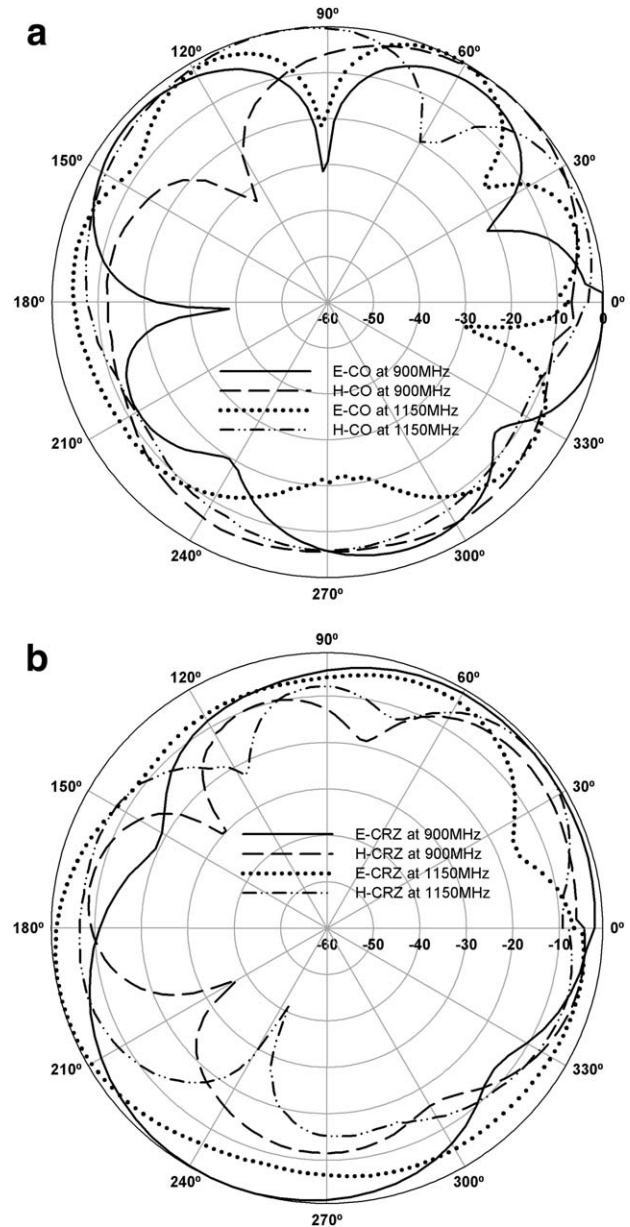


Figure 7 Measured (a) copolar radiation pattern and (b) cross polar radiation pattern at two different frequencies (1) 900 MHz and (2) 1.15 GHz

desired frequencies with any number of meandering segments. The width of the meander line is changed uniformly to study its effect on the broadband operation and is plotted in Figure 6. It is clear from the figure that the bandwidth of the antenna system varies as width (W_1) keeping the resonances same.

Hence the lower frequency resonances are due to the length of meander lines and the bandwidth is affected by the width of meander lines. Also the number of meandering segment is a key factor in determining the lowest operating frequency. It gives the flexibility to design an antenna at any resonant frequency having a particular bandwidth with a given number of segments. The antenna geometry can be truncated as and when the desired compactness, frequency of operation, and the bandwidth are obtained. The importance of the structure lies on the fact that the overall antenna system is matched for the entire band without using any external parasitic elements and without any extra

ground plane. Also the arithmetic/geometric progressive or log periodic design can improve the bandwidth capacity of the antenna. However, this increases the overall size of the antenna system.

The measured, normalized, co-polarized, and cross polarized radiation patterns in XZ plane and YZ plane at 750 MHz and 1.15 GHz are shown in Figure 7. The antenna is polarized along X direction. The efficiency of the proposed antenna is 85.7% at 1.15 GHz as measured by the Wheeler cap method [9].

After exhaustive studies, the antenna design parameters are $L_1 = 0.071\lambda_g$, $L_2 = 0.024\lambda_g$, $L_3 = 0.025\lambda_g$, $L_4 = 0.185\lambda_g$, $L_5 = 0.059\lambda_g$, $W = 0.177\lambda_g$, $W_1 = 0.029\lambda_g$, and $W_2 = 0.004\lambda_g$, where λ_g is the wavelength corresponding to f_c , $f_c = (f_l + f_h)/2$, f_l and f_h are the lower and higher -10 dB frequencies with respect to the 2:1 VSWR bandwidth. The characteristic constants of the metamaterial structure are extracted using the Matlab program governed by the equation in [10] to validate the metamaterial characteristics. It shows a negative permittivity and positive permeability at the resonances.

4. CONCLUSION

A compact broadband metamaterial-inspired planar antenna with meandered ground plane is proposed. The antenna exhibits a 2:1 VSWR bandwidth of 60.5% (0.750–1.4 GHz) without using any external parasitic components and ground. The antenna covers CDMA (824–894 MHz), GSM 800(880–960 MHz), and ISM 900(902–928 MHz) communication bands. The proposed antenna offers an area reduction of about 85% when compared to a finite ground rectangular patch antenna.

REFERENCES

1. V.I. Slyusar, Metamaterials on antenna solutions, In: International conference on antenna theory and techniques, Lviv, Ukraine, Oct 6–9, 2009, pp. 19–24.
2. Y. Rahmat-Samii, Metamaterials in antenna applications: classifications, designs and applications, In: IEEE workshop on antenna technology: Small antennas and novel metamaterials, 2006, pp.1–4.
3. R.W. Ziolkowski, Electrically small resonators: A path to efficient, electrically small antennas, In: Proceedings of Virtual Institute for Artificial Electromagnetic Materials and Metamaterials Congress, 2008, pp. 577–579.
4. A. Erentok and R.W. Ziolkowski, Efficient metamaterial-inspired electrically-small electric-based antennas: Two- and three-dimensional realizations, In: Proceedings of Antennas and Propagation Society International Symposium, Honolulu, HI, 2007, pp. 1309–1312.
5. S. Ghadarghadr, Negative permeability based electrically small antennas, IEEE Antennas Wirel Propag Lett 7 (2008), 13–17.
6. R.W. Ziolkowski, An efficient, electrically small antenna designed for VHF and UHF applications, IEEE Antennas Wirel Propag Lett 7 (2008), 217–220.
7. R.W. Ziolkowski, P. Jin, and C.-C. Lin, Metamaterial-inspired, multi-functional, near-field resonant parasitic antennas, In: IEEE International Conference on Wireless Information Technology Systems, 2010, pp. 1–4.
8. R.W. Ziolkowski, Efficient electrically small antenna facilitated by a near-field resonant parasitic, IEEE Antennas Wirel Propag Lett 7 (2008), 581–584.
9. H. Choo, R. Rogers, and H. Ling, On the wheeler cap measurement of the efficiency of microstrip antennas, IEEE Trans Antennas Propag 53 (2005), 2328–2332.
10. P.D. Imhof, R.W. Ziolkowski, and J.R. Mosig, Highly subwavelength unit cells to achieve epsilon negative (eng) metamaterial properties, IEEE Antennas and Propagation Society Symposium, Albuquerque, NM, 2006, pp. 1927–1930.

ALL-FIBER, VERSATILE FEMTOSECOND SOLITON SOURCE WITH BROAD WAVELENGTH AND REPETITION-RATE TUNING RANGES

Yizhen Wei^{1,2} and Kai Hu²

¹College of Communication Engineering, Hangzhou Dianzi University, Hangzhou 310018, China; Corresponding author: yizhenwei@hdu.edu.cn

²Centre for Optical and Electromagnetic Research, Zhejiang University, Hangzhou 310058, China

Received 26 June 2013

ABSTRACT: We demonstrate an all-fiber, widely wavelength, and repetition-rate tunable soliton source using soliton self-frequency shift (SSFS) in a single-mode fiber. A 2-ps actively mode-locked fiber laser at 1550 nm incorporating a Mach–Zehnder modulator is used as a repetition-tunable input source. The SSFS process results in a compressed, wavelength-tunable femtosecond pulse. Versatility of the source is demonstrated through tuning of soliton wavelength from 1560 to 1700 nm, as well as arbitrary pulse sequence generation. © 2014 Wiley Periodicals, Inc. Microwave Opt Technol Lett 56:613–615, 2014; View this article online at wileyonlinelibrary.com. DOI 10.1002/mop.28158

Key words: tunable; femtosecond source; soliton self-frequency shift; all fiber

1. INTRODUCTION

The femtosecond optical pulse sources have been extensively studied to achieve high pulse quality and widely tunable operation, aiming at their applications in ultrafast spectroscopy, nonlinear optics, optical chemistry, and so on. During the past decades, various mode-locked lasers [1–3] have been proposed and exploited as ultrashort pulse sources. However, a conventional mode-locked laser always suffers from limited wavelength tuning range and fixed repetition rate, because of its strictly designed cavity. To overcome these drawbacks of mode-locked lasers, several techniques have been developed, such as pulse sources based on soliton self-frequency shift (SSFS) and time-lens. After its debut in 1986 [4], the phenomenon of SSFS in optical fiber in which Raman self-pumping continuously transfer energy from the higher-frequency component to lower-frequency component has been employed to build widely wavelength-tunable femtosecond pulse sources [5–7]. In the wavelength region of anomalous dispersion, wavelength red-shift increases with both the input power and the fiber length, which provides a convenient wavelength-tuning mechanism. On the other hand, a time-lens source can generate ultrashort optical pulse with an arbitrary repetition rate. This technique achieves pulse compression by imposing a temporal quadratic phase modulation onto the incoming light [8–10] and its repetition rate is entirely decided by the radio frequency (RF) drive signal. Very recently, the combination of a time-lens source and SSFS in a large-mode-area fiber enabled a 200-fs pulse source with both wavelength and repetition rate tunabilities [11]. However, some bulk components are still required in the scheme, increasing the difficulties of alignment and daily maintenance. The use of time-lenses also introduces a series of modulators and corresponding RF devices, making the system low-energy efficiency and complex.

In this article, we build a repetition-tunable pulse generator by synchronizing a Mach–Zehnder (MZ) modulator with an actively mode-locked fiber laser (AMLFL). This scheme is all-fiber and much simpler than a time-lens source. By using the